Article

Facile Fabrication of Glycosylpyridyl-Triazole@Nickel Nanoparticles as Recyclable Nanocatalyst for Acylation of Amines in Water

Zhiwei Lin [1], Jianzhong Jin [2],*, Jun Qiao [2], Jianying Tong [2] and Chao Shen [2],*

[1] College of Petroleum Chemical Industry, Changzhou University, Changzhou 213164, China; zjsrlzw@hotmail.com

[2] College of Biology and Environmental Engineering, Zhejiang Shuren University, Hangzhou 310015, China; workhard84@126.com (J.Q.); tjy132@msn.com (J.T.)

* Correspondence: hzjjz@163.com (J.J.); shenchaozju@zjsru.edu.cn (C.S.); Tel.: +86-0571-88297172 (C.S.)

check for updates

Abstract: In this report, novel glycosylpyridyl-triazole@nickel nanoparticles (GPT-Ni) were successfully prepared via click chemistry and were fully characterized by various spectroscopy measurements. The as-prepared catalysts could be used as a recyclable catalyst for the catalytic acylation of amines by employing *N*,*N*-dimethylacetamide (DMA), *N*,*N*-dimethylpropionamide (DMP), and *N*,*N*-dimethylformamide (DMF) as acylation reagents in water, providing the corresponding amides in good yields. The practicability of this methodology is highlighted by the good recyclability of the catalyst. A unique mechanism was proposed for the catalytic process.

Keywords: glycosylpyridyl-triazole; nickel nanoparticles; nanocatalyst; acylation of amines

1. Introduction

Amides are essential components in the fine chemical industry because they are frequently encountered backbones in agricultural chemicals, pharmaceuticals, and natural products [1–3]. Traditionally, the construction of amides mainly focus on the acylation of amines by employing acyl chloride, carboxylic acid, and anhydride, as well as ester [4–6]. However, the shortcomings of these approaches suffer from low atom-economy due to the formation of many waste, the release of corrosive and volatile gases, the complex experimental operation as well as the limited stability of many acyl halides [7]. Therefore, great interest has been devoted to the development of novel catalytic approaches that would allow the highly selective and environmentally friendly preparation of amides [8–12].

Following the great progress in cross-coupling reactions using precious metal catalysts, novel methods that utilize cheap and widely abundant metals has become an important research area [13–16]. Thus, there is tremendous potential for the development of efficient approaches using non-precious metals and great demand for improving reaction scope, decreasing catalyst loading and improving catalyst stability. Compelling environmental and economical demands are thus driving chemical researchers to use more earth-abundant metals such as Fe, Co, and Ni [17]. In particular, the application of nickel catalysts in cross-coupling reactions has received considerable attention [18–27], because nickel is cheaper and more abundant than other precious metals such as Pd, Pt, and Rh. In addition, nickel has several readily available oxidation states commonly shown in catalytic process and catalytic cycles can include Ni0/NiII and NiI/NiIII cycles [28]. Therefore, the nickel-catalyzed reactions have experienced rapid advancement.

In recent years, the utilization of biomass sources such as carbohydrate, starch, cellulose and lignin also has produced great interest in the preparation of nanoparticles due to its green and essential roles in catalyzed reactions [29–33]. Recently, our group has prepared a highly active and easily recoverable heterogeneously sugar-based palladium catalysts which have been used for solvent-free Mizoroki-Heck reactions [34] and aqueous phase Suzuki-Miyaura couplings (Scheme 1a) [35]. Continuing our interests in the development of biomass-based catalyst [36], we sought to a catalytic system that would be convenient to prepare, and afford lower catalyst loading without the need of any organic ligand. Herein, we reported an efficient method for the synthesis of glycosylpyridyl-triazole@nickel nano catalysts (GPT-Ni) which were fully characterized by high resolution mass spectrum (HRMS), X-ray diffraction (XRD), infrared spectroscopy (IR), thermogravimetric analysis (TG), and transmission electron microscopy (TEM). The as-prepared catalysts were applied to catalytic acylation of amines (Scheme 1b), providing the corresponding amides in good yields.
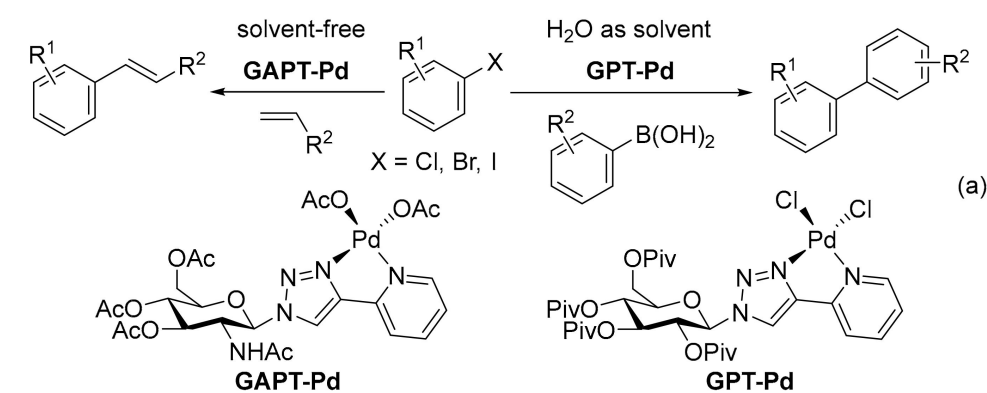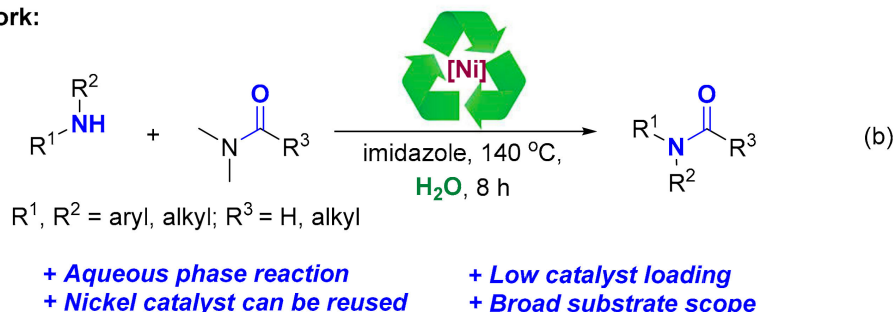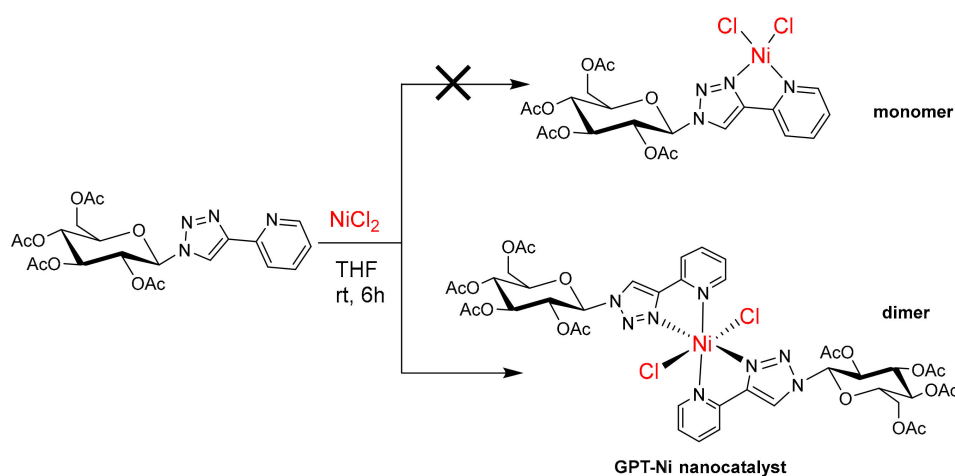

Scheme 1. The application of glycosylpyridyl-triazole@metal nanoparticles: (**a**) GAPT-Pd catalyzed Mizoroki-Heck reactions and GPT-Pd catalyzed Suzuki-Miyaura couplings; (**b**) GPT-Ni catalyzed acylation of amines.

2. Results and Discussion

The GPT-Ni nanocatalyst was synthesized using a simple and convenient approach by reacting nickel chloride with glycosyl pyridyl-triazole as ligands in tetrahydrofuran (Scheme 2). When the reaction of $NiCl_2$ (1.0 equiv.) and glycosyl pyridyl-triazole (1.2 equiv.) was set up, a GPT-Ni formulated as dimer was obtained as the sole product, which was characterized by HRMS and IR [34] (see ESI†, Figures S1 and S2). Meanwhile, if one equiv. of glycosyl pyridyltriazole ligand with two equiv. of $NiCl_2$ were mixed and stirred, only the dimer was achieved in a low yield, but nothing of monomer could be obtained. These experiments indicated that the pyridyl triazole nickel complex could easily form dimer compared to monomer, which was different to the our previously reported results [34,35]. The as-prepared catalysts were stable in air and can be stored in air for a long time. A series of characterization studies were performed to explore the possible active sites of the GPT-Ni catalyst.

The characteristic value of the catalyst was determined by X-ray photoelectron spectrographs (XPS). The Ni (2p3/2) and Ni (2p1/2) peaks were shown at 854.98 and 872.38 eV, respectively, which are the characteristic values of the Ni^{2+} (Figure 1a,b) [37]. Then the catalyst was characterized by XRD and the characteristic peak of catalyst was appeared. We can find that the characteristic values of the Ni^{2+} displacement from 15.3146 to 13.7188. The characteristic peak of sugar-based pyridyl-triazole also has obvious displacement (Figure 1c,d,e). Subsequently, the thermal stability of GPT-Ni catalyst was investigated by TG (Figure 1f). The results revealed that the catalyst remain stable up to 185 °C, suggesting that they can be used in most organic reactions with a wide temperature range. We next characterized the morphology of the as-prepared catalysts by TEM. The results demonstrated that nickel nanoparticles have a narrow size distribution with uniform and discrete spherical in shape and the average diameter of the GPT-Ni catalyst diameter was about 8–9 nm and the dispersion of the catalyst particles were very well (Figure 1g,h). The TEM image also showed that no nickel clusters were produced during the preparation.

Scheme 2. Synthesis of glycosylpyridyl-triazole@nickel nanocatalyst.

After getting the characterized catalyst, the as-prepared GPT-Ni catalyst was used to catalyze acylation of amines. We initially studied the reaction by using aniline (**1a**) and Dimethylacetamide (DMA) (**2a**) as substrate, in the presence of 1 mol% of GPT-Ni, 1 equivalent of imidazole at 140 °C under air atmosphere. The product **3a** was obtained in 35% yield (Table 1, entry 1). Meanwhile, the GAPT-Pd and GPT-Pd nanoparticles were employed as catalysts, however, no product was generated (Table 1, entries 2 and 3). Inorganic catalyst $NiCl_2$ also has a lower reactivity (Table 1, entry 4). No product was formed in the absence of metal catalyst or imidazole (Table 1, entries 5 and 6). The product was obtained in low yield when one equiv. of DMA was used (Table 1, entry 7). To our delight, the yield was significantly improved to 86% when one equiv. of sodium L-ascorbate (VC Na) was added (Table 1, entry 8). Other reductants such as $Na_2S_2O_3$ and Zn powder were used instead of VC Na, a lower isolated yield were obtained (Table 1, entries 9 and 10). Interestingly, the utilization of H_2O instead of DMA gave **3a** in 86% yield when 10 equiv. of DMA was used as acylation reagent (Table 1, entry 11). Importantly, only a slightly reduced yield was observed when the amount of the was reduced to 0.1 mol% (Table 1, entry 12). However, the yield decreased obviously when the catalyst loading was reduced to 0.05 mol%, (Table 1, entry 13). No product was obtained in the absence of GPT-Ni catalyst (Table 1, entry 14). Lowering the reaction temperature to 130 °C decreased the yield to 75% even with a prolonged reaction time, when the temperature was raised to 150 °C, the yield of **3a** have no change (Table 1, entries 15 and 16).
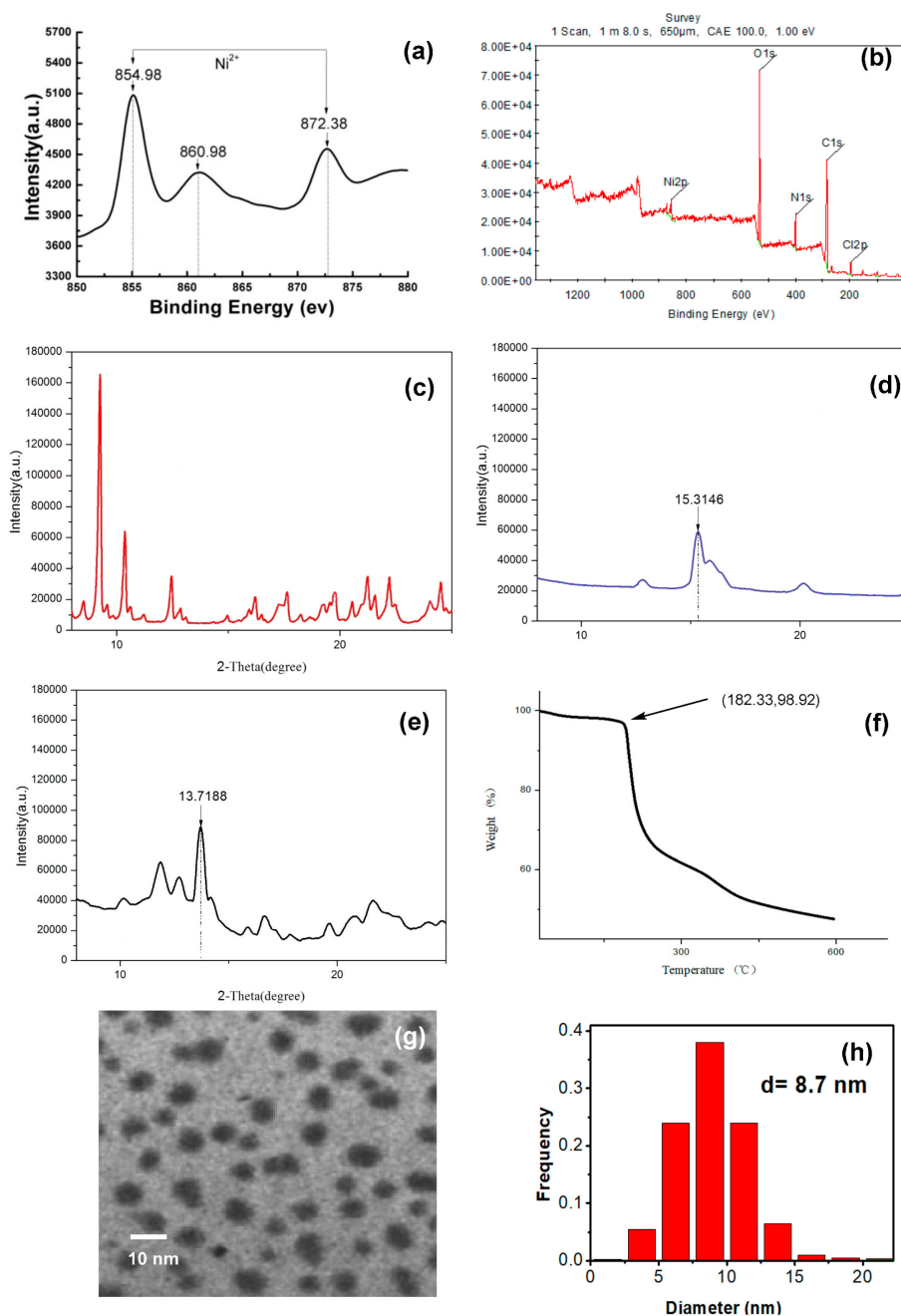
Figure 1. (**a**,**b**) XPS analysis of glycosylpyridyl-triazole@nickel nanoparticles (GPT-Ni); (**c**) XRD of GPT; (**d**) XRD of $NiCl_2$; (**e**) XRD of GPT-Ni; (**f**) thermogravimetric analysis (TG) plots of GPT-Ni; (**g**,**h**) TEM image of GPT-Ni.

After obtaining the optimized conditions, the scope of substrates was then examined, and the results were summarized in Table 2. The effect of different aryl amines was initially tested by using DMA (**2a**) as a substrate. The reactions of electron-rich and electron-deficient aryl amines with **2a** provide the desirable product **3a–3k** in good yields. These results show that the steric and electronic characters of aryl amines have no obvious effect on the *N*-acetylization reactions. We found that both aliphatic and heterocyclic amines could react with **2a** smoothly, giving corresponding products **3l–3n** in moderate to good yields. In addition, the propionylated products **3o–3q** were also obtained in satisfying yield. Notably, the substrate contains both alcohol and amine was employed and the highly selective acylated product **3r** was isolated in 68% yield.

Table 1. Reaction optimization [a].

| Entry	Catalyst (mol%)	Solvent	Reductant	Yield (%) [b]
1	GPT-Ni (1)	DMA	-	35
2	GAPT-Pd (1)	DMA	-	0
3	GPT-Pd (1)	DMA	-	trace
4	NiCl$_2$(1)	DMA	-	12
5[c]	GPT-Ni (1)	DMA	-	trace
6	-	DMA	-	0
7[d]	GPT-Ni (1)	DMA	-	17
8	GPT-Ni (1)	DMA	VC Na	86
9	GPT-Ni (1)	DMA	Na$_2$S$_2$O$_3$	26
10	GPT-Ni (1)	DMA	Zn powder	17
11[e]	GPT-Ni (1)	H$_2$O	VC Na	86
12[e]	GPT-Ni (0.1)	H$_2$O	VC Na	85
13[e]	GPT-Ni (0.05)	H$_2$O	VC Na	61
14[e]	-	H$_2$O	VC Na	0
15[e,f]	GPT-Ni (0.1)	H$_2$O	VC Na	75
16[e,g]	GPT-Ni (0.1)	H$_2$O	VC Na	85

[a] Reaction condition: **1a** (1 mmol), **2a**, catalyst (0.05–1mol%), imidazole (1 equiv.), VC Na (1 equiv.), solvent (3 mL), 140 °C for 8 h. [b] Isolated yield. [c] Without imidazole. [d] *N*,*N*-dimethylacetamide (DMA) (1 equiv.). [e] DMA (10 equiv.). [f] 130 °C, 24 h. [g] 150 °C.

Table 2. GPT-Ni catalyzed *N*-acylation of amines using DMA or *N*,*N*-dimethylpropionamide (DMP).[a,b]
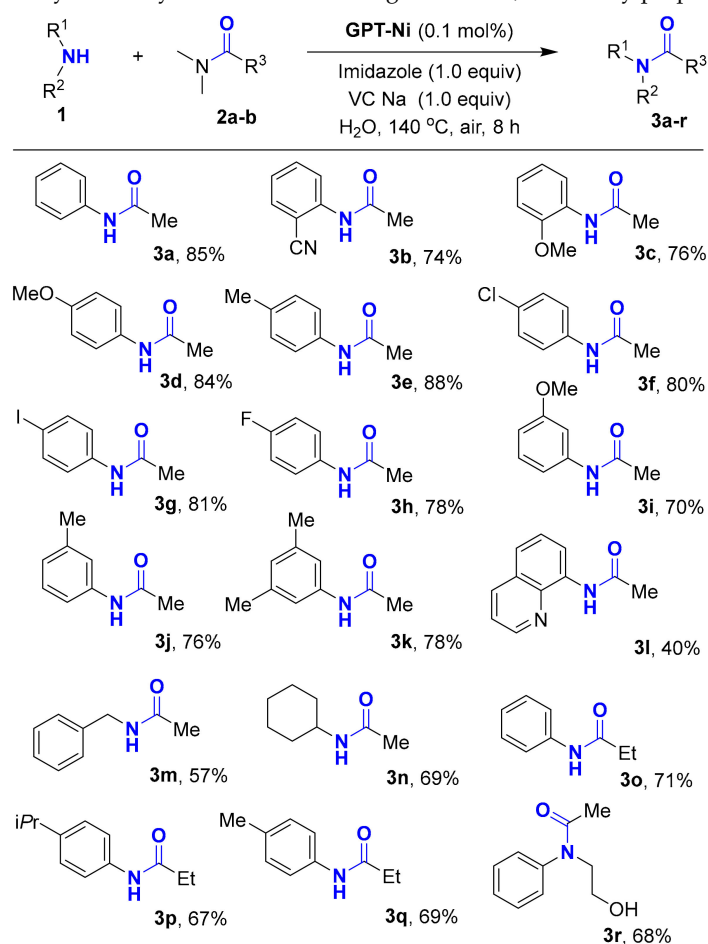

[a] Reaction conditions: **1** (1 mmol), 2 (10 equiv.), GPT-Ni (0.1 mol%), imidazole (1 equiv.), VC Na (1 equiv.), H$_2$O (3 mL), 140 °C for 8 h. [b] Isolated yield.

Encouraged by these promising results, the *N*-formylation of amines using DMF as the carbonyl source under the optimal reaction conditions was investigated (Table 3). Interestingly, the *o*, *m*-, and *p*-substituted amines gave the corresponding products in good yields. To demonstrate the synthetic application of the strategy, we applied the developed GPT-Ni catalyzed *N*-propionylation strategy to the synthesis of propanil which is a widely used contact herbicide. The reaction could afford propanil in up to 85% yield in gram scale (Scheme 3).

Table 3. GPT-Ni catalyzed *N*-formylation of amines using *N,N*-dimethylformamide (DMF).[a,b]

5a, 78%   5b, 73%   5c, 74%
5d, 78%   5e, 73%   5f, 70%
5g, 75%   5h, 75%   5i, 71%
5j, 65%   5k, 60%   5l, 67%
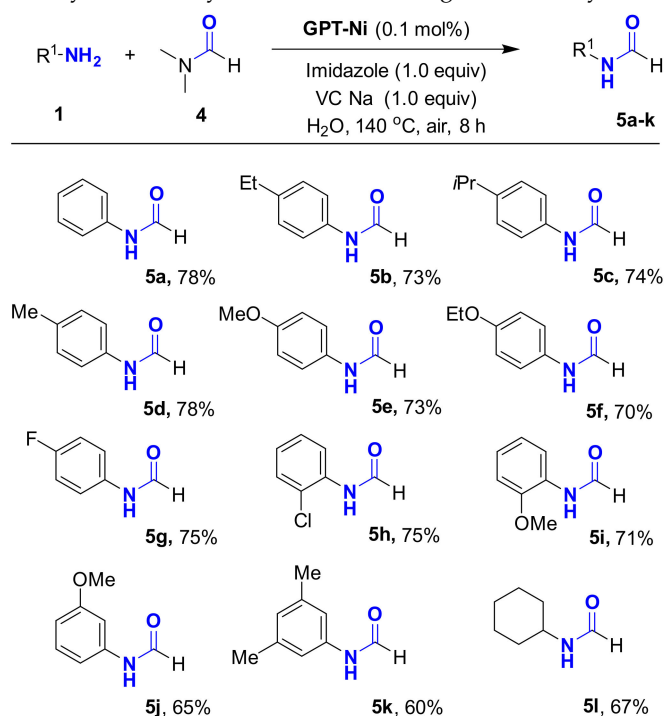
[a] Reaction conditions: **1** (1 mmol), **4** (10 equiv.), GPT-Ni (0.1 mol%), imidazole (1 equiv.), VC Na (1 equiv.), H_2O (3 mL), 140 °C for 8 h. [b] Isolated yield.
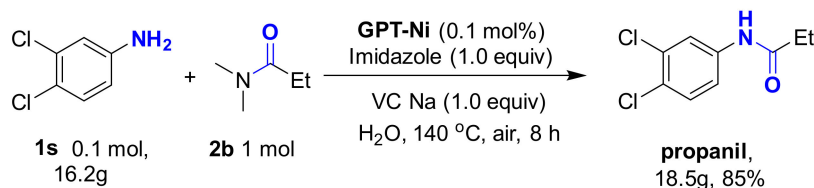
Scheme 3. Synthetic application.

The reusability of the catalyst are significant factors in practical applications of catalytic systems. To explore these problems, the feasibility of recycling the catalyst was then examined (Figure 2). When the reaction was completed, the catalyst was collected by centrifugal separation and washed with H_2O and ether twice. The corresponding amide **3a** was then dried and quantified. After drying, the retrieved catalyst was reused in the next round and the activity of the catalyst remained stable after 6 times of recycles in the reaction.

To get insights into the mechanism of GPT-Ni catalyzed acylation of amines, control experiments with selected substrates have been performed. Firstly, the acylation process could still proceed well in the presence of 2,2,6,6-tetramethyl piperidine-1-oxyl (TEMPO) (Scheme 4a). This result clearly shows that a free radical process was not involved in the reaction. Then, the reaction was performed by using acetylimidazole (**6**) as acylation agent directly, an excellent yield of product up to 90% was

obtained (Scheme 4b). This result explains that the compound **6** is an important intermediate in this transformation.
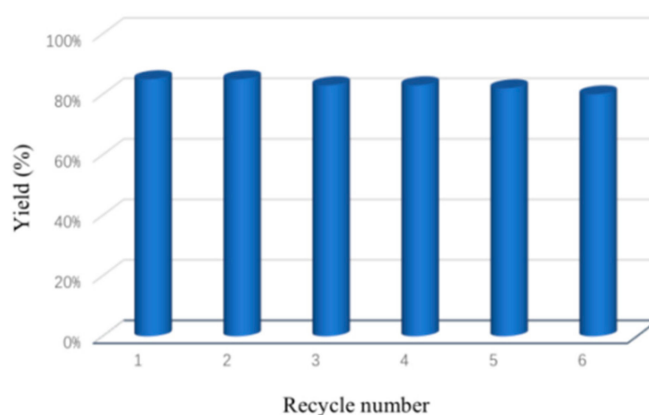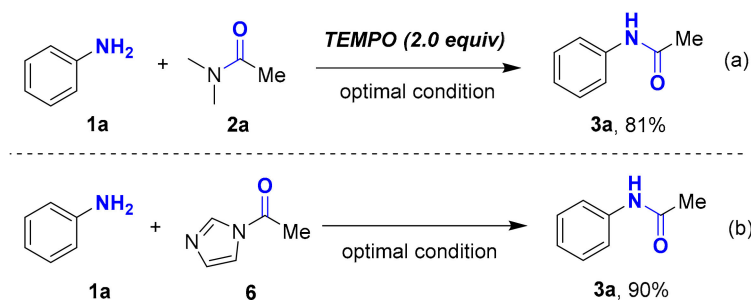

Figure 2. Catalyst recycling.

Scheme 4. Mechanism study: (**a**) Free radical experiment; (**b**) Acetylimidazole (**6**) as acylation agent directly.

Based on the results above, a plausible mechanism was proposed as shown in Figure 3. The GPT-Ni catalyst plays a dual role in this reaction. Firstly, GPT-NiII was reduced to GPT-Ni^0 in the presence of VC Na which used as a reductant. The generated GPT-Ni^0 inserted into the C–N bond of DMA to form complex **A** though oxidative addition. Then, complex **A** was converted to complex **B** via ligand exchange. Subsequent reductive elimination provided the important intermediate acetylimidazole (**6**). Nextly, GPT-Ni^{II} used as Lewis acid to coordinate with acetylimidazole (**4**) to form complex **C**. Then, nucleophilic attack of amine (**1**) on complex **C** provides complex **D** followed by the release of imidazole that leads to the generation of complex **E**. Finally, target product **3** is obtained via a metal dissociation process.
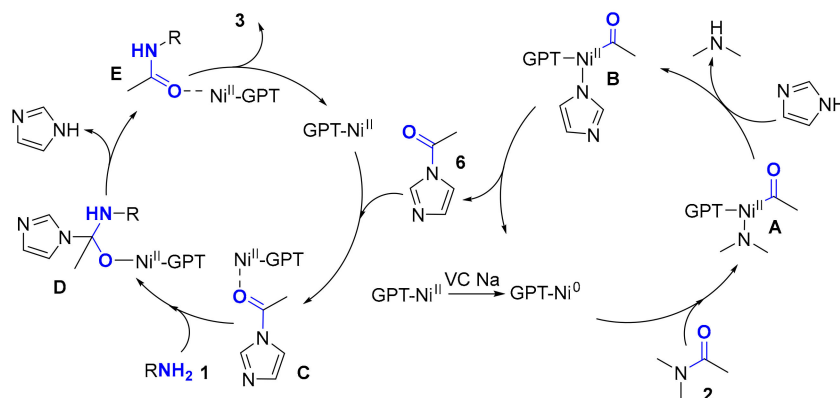

Figure 3. Plausible Mechanism.

3. Experimental Materials

All the chemicals were purchased commercially and used without further purification. All acylated products were isolated by short chromatography on a silica gel (200–300 mesh) column using petroleum ether (60–90 °C) and ethyl acetate. ^{1}H and ^{13}C Nuclear Magnetic Resonancespectra were recorded on a Bruker Advance 500 spectrometer (Swiss Brüker, Hangzhou, China)at ambient temperature with chloroform-*d* as solvent and tetramethylsilane (TMS) as the internal standard. Analytical thin layer chromatography (TLC) was performed on Merkprecoated TLC (silica gel 60 F254) plates which were supplied by Aladdin (Shanghai, China). Transmission electron microscopy (TEM) images were taken on FEI T20 microscope (FEI, Shanghai, China). The small-angle X-ray diffraction (SAXRD) data were taken on a German Bruker D4 X-ray diffractometer with Niltered Cu Ka radiation (40 kV, 40 mA) (Swiss Brüker, Hangzhou, China). Thermogravimetric analyses were performed with a SII Nano Technology EXTAR TG/DTA7220 thermal analyzer at 10 °C/min in nitrogen atmosphere (10 mL/min). Then, 5 mg of each sample in an alumina pan was analyzed in the 40–600 °C temperature range. X-ray photoelectron spectrographs (XPS) were determined with an Axis Ultra DLD electron spectrometer (Kratos Analytical, Manchester, UK) with the C1s = 284.8 eV signal as the internal standard. Compounds for HRMS were analyzed by positive mode electrospray ionization (ESI) using Agilent 6530 Quadrupole-Time of Flight mass spectrometer (Agilent, Shanghai, China). All glycosyl pyridyl-triazoles were prepared according to our previous papers. [35]

3.1. General Procedure for Synthesis of Glycosyl Pyridyl-Triazole@nickel Catalysts

Synthesis of GPT-Ni catalyst: $NiCl_2$ (0.50 mmol) was dissolved in anhydrous tetrahydrofuran (20 mL) and glycosyl pyridyl-triazole (0.60 mmol) was added. The solid-liquid mixture was reacted for 6–8 h at 25 °C, then add ether, the turquoise precipitate slowly appeared and after which the product was filtered, washed thoroughly with large volume of ether in order to remove any adsorbed nickel and then dried at 30 °C under vacuum. The nanoparticle catalyst was obtained as turquoise powder.

3.2. General Procedure for N-acylation of Amines in Water

To a 15 mL reaction tube charged with water (3 mL) was added with **1** (1 mmol), DMA, DMP, or DMF (10 equiv.), GPT-Ni catalyst (0.1 mol%), imidazole (1 mmol), and sodium L-ascorbate (1 mmol). Then the mixture was stirred at 140 °C under air for 8 h. After completion of the reaction, the mixture was allowed to cool down to 25 °C. Then the reaction aqueous phase was extracted with ethyl acetate for 3 times (3 × 5 mL). The combined organic layers were dried over anhydrous Na_2SO_4, concentrated under vacuum, and then purified by column chromatography (n-hexane/ethyl acetate 10:1) to afford the desired products.

3.3. Catalyst Recovery Experiment

A 15 mL reaction tube charged with water (1 mL) was added with **1** (1 mmol), **2** (10 equiv.), GPT-Ni catalyst (0.1 mol%), imidazole (1 mmol), and sodium L-ascorbate (1 mmol). Then the mixture was stirred at 140 °C under air for 8 h. After completion of the reaction, the catalyst was collected by centrifugal separation and washed with H_2O and ether twice. Then the catalyst was dried at 70 °C for 6 h. The separated catalyst was recharged with a fresh substrate for the next round.

4. Conclusions

In conclusion, we have developed a simple and highly active catalytic system for efficient acylation of amines by employing DMA, DMP, and DMF as acylation reagent using a catalytic amount (as low as 0.1 mol%) of GPT-Ni catalyst and in water. The activity of catalyst remains stable after six times of recycles, which makes it to be an economical and practical tool for the synthesis of amides. The GPT-Ni catalyst plays a dual role in this transformation and a unique mechanism was proposed for the catalytic process. In addition, the marketed herbicide propanil could be easily synthesized using this protocol.

References

1. Pattabiraman, V.R.; Bode, J.W. Rethinking amide bond synthesis. *Nature* **2011**, *480*, 471–479. [CrossRef]

2. Alcaide, B.; Almendros, P.; Aragoncillo, C. β-Lactams: Versatile Building Blocks for the Stereoselective Synthesis of Non-β-Lactam Products. *Chem. Rev.* **2007**, *107*, 4437–4492. [CrossRef]

3. Patre, R.E.; Mal, S.; Nilkanth, P.R.; Ghorai, S.K.; Deshpande, S.H.; Qacemi, M.E.; Smejkal, T.; Pal, S.; Manjunath, B.N. First report on bio-catalytic N-formylation of amines using ethyl formate. *Chem. Commun.* **2017**, *53*, 2382–2385. [CrossRef]

4. Pasqua, A.E.; Matheson, M.; Sewell, A.L.; Marquez, R. Fast, Economic, and Green Synthesis of N-Formylated Benzotriazoles. *Org. Process Res. Dev.* **2011**, *15*, 467–470. [CrossRef]

5. Sawant, D.N.; Bagal, D.B.; Ogawa, S.; Selvam, K.; Saito, S. Diboron-Catalyzed Dehydrative Amidation of Aromatic Carboxylic Acids with Amines. *Org. Lett.* **2018**, *20*, 4397–4400. [CrossRef] [PubMed]

6. Hie, L.; Nathel, N.F.F.; Hong, X.; Yang, Y.F.; Houk, K.N.; Garg, N.K. Nickel-Catalyzed Activation of Acyl C-O Bonds of Methyl Esters. *Angew. Chem. Int. Ed.* **2016**, *55*, 2810–2814. [CrossRef] [PubMed]

7. Dunetz, J.R.; Magano, J.; Weisenburger, G.A. Large-Scale Applications of Amide Coupling Reagents for the Synthesis of Pharmaceuticals. *Org. Process Res. Dev.* **2016**, *20*, 140–177. [CrossRef]

8. Nasrollahzadeh, M.; Motahharifar, N.; Sajjadi, M.; Aghbolagh, A.M.; Shokouhimehr, M.; Varma, R.S. Recent advances in N-formylation of amines and nitroarenes using efficient (nano)catalysts in eco-friendly media. *Green Chem.* **2019**, *21*, 5144–5167. [CrossRef]

9. Chen, B.C.; Bednarz, M.S.; Zhao, R.; Sundeen, J.E.; Chen, P.; Shen, Z.Q.; Skoumbourdis, A.P.; Barrish, J.C. A new facile method for the synthesis of 1-arylimidazole-5-carboxylates. *Tetrahedron Lett.* **2000**, *41*, 5453–5456. [CrossRef]

10. Zhang, Y.; Wang, H.; Yuan, H.; Shi, F. Hydroxyl Group-Regulated Active Nano-Pd/C Catalyst Generation via in Situ Reduction of Pd(NH$_3$)xCly/C for N-Formylation of Amines with CO$_2$/H$_2$. *ACS Sustain. Chem. Eng.* **2017**, *5*, 5758–5765. [CrossRef]

11. Gunanathan, C.; Ben-David, Y.; Milstein, D. Direct synthesis of amides from alcohols and amines with liberation of H$_2$. *Science* **2007**, *317*, 790–792. [CrossRef] [PubMed]

12. Sonawane, R.B.; Rasal, N.K.; Bhange, D.S.; Jagtap, S.V. Copper-(II) Catalyzed N-Formylation and N-Acylation of Aromatic, Aliphatic, and Heterocyclic Amines and a Preventive Study in the C-N Cross Coupling of Amines with Aryl Halides. *ChemCatChem* **2018**, *10*, 3907–3913. [CrossRef]

13. Tasker, S.Z.; Standley, E.A.; Jamison, T.F. Recent advances in homogeneous nickel catalysis. *Nature* **2014**, *509*, 299–309. [CrossRef] [PubMed]

14. Ananikov, V.P. Nickel: The "Spirited Horse" of Transition Metal Catalysis. *ACS Catal.* **2015**, *5*, 1964–1971. [CrossRef]

15. Rudolph, A.; Lautens, M. Secondary Alkyl Halides in Transition-Metal-Catalyzed Cross-Coupling Reactions. *Angew. Chem. Int. Ed.* **2009**, *48*, 2656–2670. [CrossRef]

16. Ying, B.; Xu, J.; Zhu, X.; Shen, C.; Zhang, P. Catalyst-controlled selectivity in the synthesis of C2- and C3-sulfonate esters from quinoline N-oxides and aryl sulfonyl chlorides. *ChemCatChem* **2016**, *8*, 2604–2608. [CrossRef]

17. Gandeepan, P.; Müller, T.; Zell, D.; Cera, G.; Warratz, S.; Ackermann, L. 3d Transition Metals for C-H Activation. *Chem. Rev.* **2019**, *119*, 2192–2452. [CrossRef]

18. Rosen, B.M.; Quasdorf, K.W.; Wilson, D.A.; Zhang, N.; Resmerita, A.-M.; Garg, N.K.; Percec, V. Nickel-Catalyzed Cross-Couplings Involving Carbon-Oxygen Bonds. *Chem. Rev.* **2011**, *111*, 1346–1416. [CrossRef]

19. Sonawane, R.B.; Rasal, N.K.; Jagtap, S.V. Nickel-(II)-Catalyzed N-Formylation and N-Acylation of Amines. *Org. Lett.* **2017**, *19*, 2078–2081. [CrossRef]

20. Liu, X.; Jia, J.; Rueping, M. Nickel-Catalyzed C-O Bond-Cleaving Alkylation of Esters: Direct Replacement of the Ester Moiety by Functionalized Alkyl Chains. *ACS Catal.* **2017**, *7*, 4491–4496. [CrossRef]

21. Han, F.S. Transition-metal-catalyzed Suzuki–Miyaura cross-coupling reactions: A remarkable advance from palladium to nickel catalysts. *Chem. Soc. Rev.* **2013**, *42*, 5270–5298. [CrossRef]

22. Li, S.; Gong, J. Strategies for improving the performance and stability of Ni-based catalysts for reforming reactions. *Chem. Soc. Rev.* **2014**, *43*, 7245–7256. [CrossRef]

23. Pu, X.; Hu, J.; Zhao, Y.; Shi, Z. Nickel-Catalyzed Decarbonylative Borylation and Silylation of Esters. *ACS Catal.* **2016**, *6*, 6692–6698. [CrossRef]

24. Hie, L.; Nathel, N.F.F.; Shah, T.K.; Baker, E.L.; Hong, X.; Yang, Y.-F.; Liu, P.; Houk, K.N.; Garg, N.K. Conversion of amides to esters by the nickel-catalysed activation of amide C-N bonds. *Nature* **2015**, *524*, 79–83. [CrossRef]

25. Beutner, G.L.; Hsiao, Y.; Razler, T.; Simmons, E.M.; Wertjes, W. Nickel-Catalyzed Synthesis of Quinazolinediones. *Org. Lett.* **2017**, *19*, 1052–1055. [CrossRef]

26. Hansen, E.C.; Pedro, D.J.; Wotal, A.C.; Gower, N.J.; Nelson, J.D.; Caron, S.; Wei, D.J. New ligands for nickel catalysis from diverse pharmaceutical heterocycle libraries. *Nat. Chem.* **2016**, *8*, 1126–1130. [CrossRef]

27. Xu, J.; Qiao, L.; Shen, J.; Chai, K.; Shen, C.; Zhang, P.F. Nickel(II)-Catalyzed Site-Selective C-H Bond Trifluoromethylation of Arylamine in Water through a Coordinating Activation Strategy. *Org. Lett.* **2017**, *19*, 5661–5664. [CrossRef]

28. Harry, N.A.; Saranya, S.; Ujwaldev, S.M.; Anilkumar, G. Recent advances and prospects in nickel-catalyzed C–H activation. *Catal. Sci. Technol.* **2019**, *9*, 1726–1743. [CrossRef]

29. Polshettiwar, V.; Luque, R.; Fihri, A.; Zhu, H.; Bouhrara, M.; Basset, J.M. Magnetically Recoverable Nanocatalysts. *Chem. Rev.* **2011**, *111*, 3036–3075. [CrossRef]

30. Shen, C.; Zhang, P.F. D-Glucosamine-derived Chiral Catalysts for Asymmetric Reactions. *Curr. Org. Chem.* **2013**, *17*, 1507–1524. [CrossRef]

31. Baig, R.B.N.; Varma, R.S. A highly active and magnetically retrievable nanoferrite-DOPA-copper catalyst for the coupling of thiophenols with aryl halides. *Chem. Commun.* **2012**, *48*, 2582–2584. [CrossRef]

32. Shen, C.; Xu, J.; Yu, W.; Zhang, P. A highly active and easily recoverable chitosan@copper catalyst for the C–S coupling and its application in the synthesis of zolimidine. *Green Chem.* **2014**, *16*, 3007–3012. [CrossRef]

33. Molnár, Á. The use of chitosan-based metal catalysts in organic transformations. *Coordin. Chem. Rev.* **2019**, *388*, 126–171. [CrossRef]

34. Shen, C.; Shen, H.; Yang, M.; Xia, C.; Zhang, P. A novel d-glucosamine-derived pyridyl-triazole@palladium catalyst for solvent-free Mizoroki-Heck reactions and its application in the synthesis of Axitinib. *Green Chem.* **2015**, *17*, 225–230. [CrossRef]

35. Shen, H.Y.; Shen, C.; Chen, C.; Wang, A.; Zhang, P. Novel glycosyl pyridyl-triazole@palladium nanoparticles: Efficient and recoverable catalysts for C-C cross-coupling reactions. *Catal. Sci. Technol.* **2015**, *5*, 2065–2071. [CrossRef]

36. Shen, C.; Xu, J.; Ying, B.; Zhang, P. Heterogeneous chitosan@copper(II)-catalyzed remote trifluoromethylation of aminoquinolines with the Langlois reagent by radical cross-coupling. *ChemCatChem* **2016**, *8*, 3559. [CrossRef]

37. Zhang, Y.M.; Yang, H.M.; Chi, Q.; Zhang, Z.Z. Nitrogen-doped carbon-supported nickel nanoparticles: A robust catalyst to bridge the hydrogenation of nitriles and the reductive amination of carbonyl compounds for the synthesis of primary amines. *ChemSusChem* **2019**, *12*, 1246–1255. [CrossRef]